Assessing Miles Ridge landslide activity using an integrated ground-RPAS-satellite approach

John Stix and Justin Roman*
Department of Earth and Planetary Sciences, McGill University

Margaret Kalacska and Oliver Lucanus
Applied Remote Sensing Laboratory (ARSL), Department of Geography, McGill University

Panya S. Lipovsky
Yukon Geological Survey

Pablo Arroyo-Mora
National Research Council of Canada, Flight Research Laboratory

Stix, J., Roman, J., Kalacska, M., Lucanus, O., Lipovsky, P.S. and Arroyo-Mora, P., 2026. Assessing Miles Ridge landslide activity using an integrated ground-RPAS-satellite approach. *In:* Yukon Exploration and Geology 2025, A. Stuart, L.H. Weston and S.K. Schultz (eds.), Yukon Geological Survey, Government of Yukon, p. 221–237.

Abstract

The Miles Ridge landslide in southwest Yukon presents a potential hazard to the nearby White River bridge along the Alaska Highway. To assess the current behaviour and stability of this landslide, we integrated ground-based GNSS surveying, Drone-In-a-Box (DIAB) 3D modelling, and Sentinel-1 InSAR analysis. A ground survey in 2025 identified active tension cracks and widespread loss of the original 2007 GNSS markers, indicating continued deformation at the ridge crest. Five DIAB-derived surface models captured localized but substantial erosion and deposition within the central amphitheatre and lower channel system of the landslide, resulting in measurable volumetric change over a two-month interval (July–September). Over a one-month period (July–August), the DIAB models showed an apparent loss of debris from much of the landslide surface. Differential InSAR (DInSAR) analysis from 2017 to 2024 may indicate long-term subsidence across the landslide. Together, these datasets reveal an actively, but slowly evolving slope characterized by geomorphic change and persistent instability, underscoring the importance of continued monitoring to evaluate future movement and potential impacts to the Alaska Highway.

Plain language summary

The Miles Ridge landslide is an area of active ground movement in the Nutzotin Mountains, a small mountain range at the northern extent of the St. Elias Mountains. Located only a few kilometres from the Alaska Highway and the White River bridge, the landslide poses a potential threat to this critical infrastructure. To better understand the behaviour and current activity of the landslide, we conducted a series of ground-based, RPAS-based (drone), and satellite-based studies in the summer of 2025. We installed a new series of markers near the crest of Miles Ridge and surveyed them during one day of fieldwork. The markers are located in a zone of actively forming tension cracks and will be resurveyed in the future at periodic intervals. Using RPAS and satellite imagery, we mapped out different zones in the landslide's upper and lower parts. The upper part is dominated by a large talus apron which appears to supply material into the lower reaches of the landslide. The lower part is divided

* john.stix@mcgill.ca

into a series of lobes separated by erosional gullies. During the two-month survey, the lower zone experienced both localized debris erosion and accumulation. We also imaged the fan area where debris from the landslide drainage enters the White River several hundred metres upstream from the bridge. Our satellite measurements suggest that the Miles Ridge landslide appears to be moving over time, highlighting the need for further work to evaluate impacts to the Alaska Highway.

Introduction

Natural hazards are an increasing concern for local communities and for territorial, provincial and state governments. They also pose challenges at both national and global scales. From 1980 to 2000, annual global losses from natural disasters never exceeded US$200 billion on an inflation-adjusted basis. Since 2000, this level of loss has frequently been surpassed (Munich RE, 2025). The key issue is twofold: first, residential and commercial structures continue to be constructed in vulnerable areas with insufficient regard to hazard evaluations or hazard maps; and second, the changing global climate is increasing both the frequency and severity of naturally hazardous weather-related events, such as hurricanes (e.g., Holland and Bruyère, 2014), floods (e.g., Hirabayashi et al., 2013), and landslides (e.g., Gariano and Guzzetti, 2016). The problem is accentuated at high latitudes where the rate of warming is greater than at low and mid-latitudes. In northern Canadian environments, such as the Yukon and Northwest Territories, these changes are most evident in the cryosphere, manifesting as increased coastal erosion (e.g., Irrgang et al., 2018), permafrost melting (e.g., Burn and Zhang, 2009), and glacier surges and ice dam formation (e.g., Kochtitzky et al., 2020).

In the Yukon, natural hazards can have a profound impact on critical infrastructure, including highways and railways. An example of such critical infrastructure is the Alaska Highway, which extends 892 km across the Yukon from Watson Lake in the south, to north of Beaver Creek and the Alaska border. This highway is the most heavily used transportation route in the Yukon, and it is also the principal road linking Alaska with the contiguous United States. As such, it serves as one of North America's most important transportation links.

The Alaska Highway is subject to a variety of hazards that can disturb its road surface, including earthquakes, flooding, permafrost melting and wildfires. At kilometre 1818.5, near Koidern, the highway crosses the White River, a major tributary draining the St. Elias Mountains, by means of the White River bridge. An active zone of mass movement, named the Miles Ridge landslide, is located at the head of an unnamed drainage that flows into the White River about 500 m upstream of this bridge (Fig. 1). Since the early 1990s, relatively small-scale rockfall, slumping, and debris flow activity near the crest of Miles Ridge has caused unconsolidated material to accumulate in the upper part of the drainage over 500 vertical metres above the river (Bond et al., 2008). The toe of the landslide is located ~1.4 km from the bridge. Should this debris or any underlying unstable rock masses become mobilized in a larger-scale event, there is potential for it to deflect the White River and cause undermining of the bridge structure or impact the bridge directly. Any damage to the highway or bridge could have significant repercussions for the Yukon and beyond, including Alaska, the contiguous United States and the provinces of British Columbia and Alberta.

The purpose of this contribution is to present new results from ground-based, remotely piloted aircraft system (RPAS or drone), and satellite data of the Miles Ridge landslide and surrounding area, in order to better understand its current behaviour and to gain new insight into potential future movements of the landslide. We first present results from ground-based, RPAS and satellite data, and then discuss their significance and implications to provide an integrated view of the Miles Ridge landslide system at a variety of spatial scales.

Study area

Miles Ridge is located approximately 6 km west of Koidern, Yukon, in the Nutzotin Mountains, a small mountain range at the northern extent of the St. Elias Mountains. The ridge crest is at an elevation of ~1480 m above sea level (ASL) and forms a ~400 m-wide headscarp in the landslide source zone. The landslide covers an area of ~13 ha, extends ~580 m horizontally, and drops ~370 m vertically on a steep (~34°) northeast-facing slope. The White River floodplain is at an elevation of ~700 m at the White River bridge (Fig. 1).

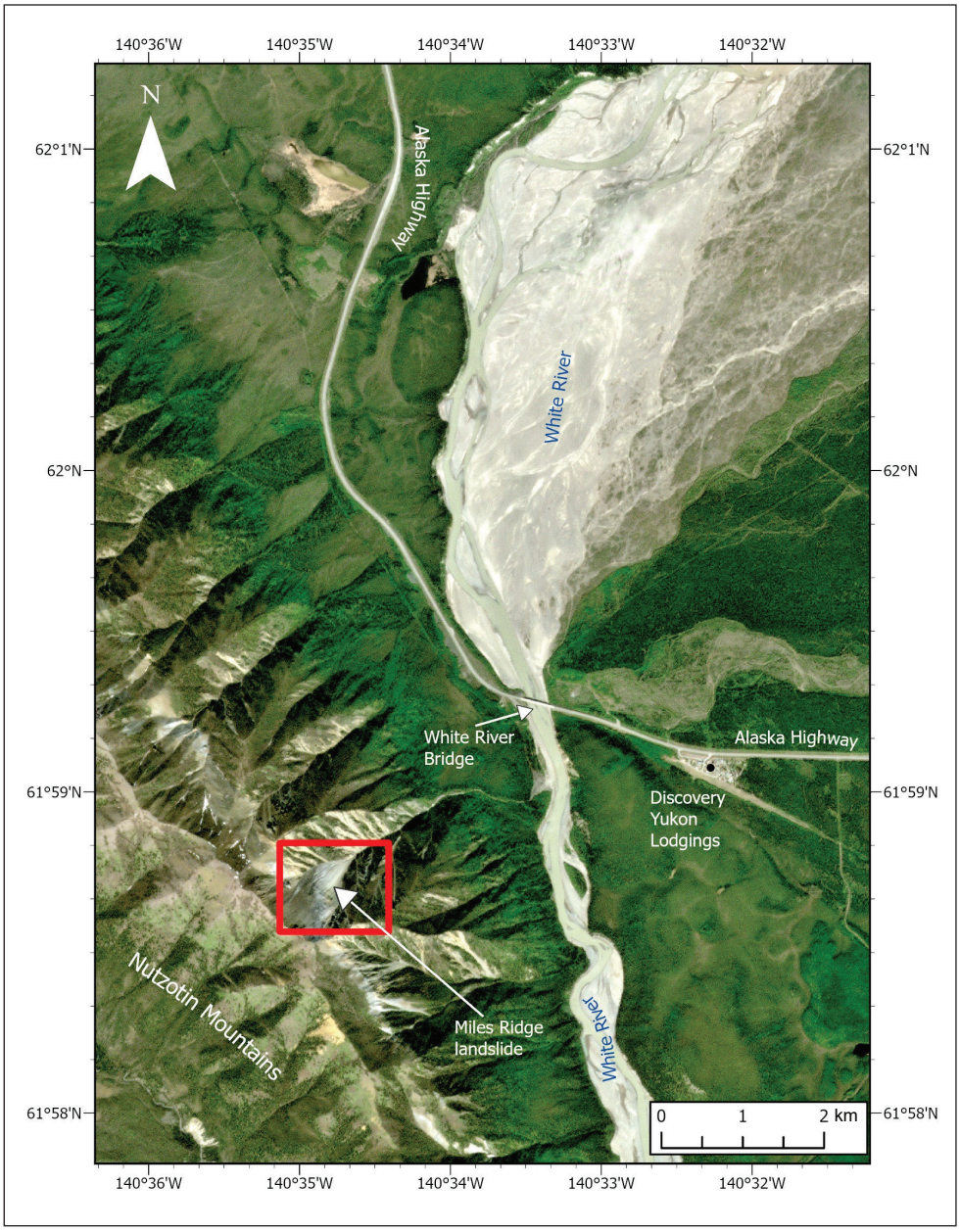

Figure 1. *Location map of the Miles Ridge landslide and surrounding area. The study area is outlined in red.*

The region is geologically very active, owing to steep rugged slopes, permafrost degradation, weak local lithologies, and high regional seismicity (Han et al., 2024). This elevated level of seismicity is exemplified by the M7.0 earthquake and subsequent aftershocks that occurred in December 2025 along the strike-slip Connector fault, 188 km south of Miles Ridge. The Denali fault is another crustal-scale, strike-slip fault which extends in a northwest-southeast direction at the foot of Miles Ridge to the north (Bender and Haeussler, 2017). Although a M7.9 earthquake on the Denali fault occurred in 2002, approximately 400 km to the northwest, the part of the fault at Miles Ridge is located along what is referred to as the Eastern Denali fault (EDF), which has experienced lower seismicity and slip rates than other parts of the fault farther to the west (Haeussler et al., 2017; Marechal et al., 2018). No earthquakes large enough to generate surface ruptures have occurred along the EDF for at least 500 years (Clague, 1979), but Blais-Stevens et al. (2020) determined that up to four >M6 earthquakes have occurred along the EDF in the last 6000 years (Finley et al., 2022).

The landslide source zone is controlled by complex fault-bounded structural geology. Relatively resistant volcanic rocks of the Station Creek Formation buttress extremely incompetent overlying units, including highly altered, clay-rich Kluane ultramafic rocks and Nikolai formation basalts (Bond et al., 2008). Ongoing deformation of these overlying rocks has likely been triggered by partial collapse of the supporting Station Creek Formation rocks.

As further erosion and accumulation of debris occur in the landslide initiation zone, the supporting volcanic rocks are becoming increasingly loaded. This, in combination with the fact that the landslide is located within a region of high seismicity, suggests that the southeast side of the basin will eventually collapse. The consequences of such a failure would vary depending on the seasonal timing, event magnitude, and runout distance of the debris (Bond et al., 2008).

Methodology

Ground measurements

In 2007, forty-eight wooden stakes and rebar monuments were installed and surveyed on the Miles Ridge landslide (Bond et al., 2008), extending along the headscarp and across three transects on the middle and lower sections of the slide. These were installed to facilitate potential future ground deformation monitoring efforts, although no subsequent survey results were ever reported. The site was visited by helicopter on July 9, 2025, to locate and resurvey any remaining stakes and document current ground conditions. Due to safety concerns, the middle and lower sections of the slide could not be accessed by foot; consequently none of the 2007 stakes on the lower three transects could be located on the ground, nor were any visible from the helicopter.

On the crest of Miles Ridge, along the landslide headscarp, only one of the original wooden stakes from the 2007 survey could be located (L102). Only a fragment of this stake remained, so it was replaced with rebar and resurveyed. Twelve new stakes for a GPS-GNSS survey were then installed along a ~110 m transect on an unstable slope encompassing several tension cracks at the northwestern end of the headscarp (Fig. 2). This new transect, termed the MR transect (see below), was oriented in a northwest-southeast line, and the stakes were placed approximately 12 m apart. The new stakes included both wooden stakes and rebar to ensure long-term durability and accessibility.

A two-part GNSS receiver and base station setup was used for this survey. The base station (D-RTK 3 Multifunctional Station; DJI, Shenzhen, China) was temporarily set up on the northern side of the airstrip at Discovery Yukon Lodgings on July 9, 2025. It logged

Figure 2. *Photograph facing southeast illustrating the new MR line of wood and rebar markers installed on July 9, 2025. The markers are spaced approximately 12 m apart. Note person for scale in upper part of image.*

raw GNSS observations continuously throughout the survey on Miles Ridge, which was approximately 2.5 km west of the base station. An Emlid Reach RS2 (Emlid Tech Kft, Budapest, Hungary) receiver was used as the rover to survey all points. The Emlid Flow application on an iPhone 14 Pro Max was used to operate the RS2. The RS2 was set to log GNSS observations continuously from 1255 to 1613 hours local time (1955 to 2313 hours UTC). At each stake, the rover was held stationary for one minute and the locations were recorded through a Survey Project. This method of collection, called stop-and-go, allows for the positions where the rover was stationary to be extracted from the raw logs in post processing. For the naming convention, the resurveyed 2007 Yukon Geological Survey (YGS) point was labeled using its original ID with the suffix '-new' (i.e., L102–new), whereas the newly installed markers were assigned the prefix 'MR' for Miles Ridge, followed by sequential numbers (e.g., MR-01, MR-02, etc.).

After the data collection on the ridge was completed, the base station's raw GNSS observations were converted to standard RINEX files with Emlid Studio v.1.9 (Emlid Tech Kft, Budapest, Hungary) and uploaded to Natural Resources Canada's (NRCAN) Precise Point Positioning (PPP) service (Government of Canada, 2025) to obtain its accurate position. A single-point GNSS solution would only provide metre-level accuracy, whereas PPP applies satellite orbit, clock, and bias corrections to achieve centimetre-level accuracy.

To calculate the positions of the stakes, a post-processed kinematic (PPK) methodology was used. To do so, Emlid Studio v.1.9 was used with the RS2 rover's raw logs and the exported survey positions. The base station's position determined through the PPP processing was also input. This PPK workflow allows for corrections of the rover's GNSS data to improve position accuracy. The outputs from the workflow were latitude, longitude and ellipsoidal height of each location where the RS2 rover was stationary for one minute (also where the survey points were recorded in the Emlid Flow application). Coordinates reported in 2007 for the L102 stake were compared to its position acquired in 2025.

RPAS measurements

The DJI Dock 2 is a compact (~34 kg), fully integrated drone-in-a-box (DIAB) system designed to enable routine, automated RPAS operations with minimal on-site human involvement. The system pairs a weather-resistant docking station equipped with environmental monitoring, automated battery charging, and internal thermal regulation with the DJI Matrice 3D/3TD aircraft, allowing remotely scheduled missions (Fig. 3). For this deployment, the Dock 2 was mounted onto a reinforced wooden base installed on top of a shipping container, providing a secure, elevated platform with stable AC power and hard-wired Ethernet connectivity from a Starlink (a low-orbit satellite-based internet system operated by SpaceX). The installation was located 2.55 km from the ridge crest, the farthest point of the area being monitored. The DJI Mavic 3TD (M3TD) aircraft used here with the Dock 2 integrates three onboard imaging sensors, including a 48 MP wide-angle RGB camera (1/1.32-inch CMOS) that served as the primary mapping instrument due to its RTK-precision geotagging. It also includes a 12 MP telephoto RGB camera and a calibrated thermal infrared sensor with ≤50 mK sensitivity, enabling multi-modal imaging and enhanced situational awareness. The aircraft features six-direction obstacle sensing, ADS-B AirSense capability, a maximum operating range of 10 km, and a maximum flight speed of 15 m/s.

Flight planning was carried out using DJI FlightHub 2, where a custom waypoint-based mission design kept the aircraft within the Canadian legal altitude limits by following terrain-constrained paths across the

Figure 3. *Installation of the DJI Dock 2 on the top of the shipping container; Miles Ridge is in the distance. The inset illustrates the M3TD during take-off. The Dock 2 weighs 34 kg and is 57 × 58.3 × 46.5 cm (L×W×H) with the doors closed.*

landslide surface and transit between the Dock 2 and the survey area. FlightHub 2's information security management system is ISO/IEC 27001 certified ensuring confidentiality, information integrity, and data availability. The installation and flight planning are detailed in Kalacska et al. (2026).

A total of five 3D models of the Miles Ridge landslide were generated between July 13 and September 7, 2025 using the online processing option within FlightHub 2. The last two flights were conducted with the pilot-in-command operating the system remotely from eastern Canada, approximately 4000 km from the installation location (with a local visual observer). Given the distance of the landslide from the installation, the performance of the Dock 2 RTK system, and the accuracy of the Dock 2 calibration at the time of installation (estimated from Natural Resources Canada's Precise Point Positioning service), the combined expected uncertainty of the real-world positioning of the models is approximately 3.56-4.56 cm horizontally and 5.06 cm vertically at the farthest point. Multi-temporal cross-section and volume change analyses were carried out in FlightHub 2 with the Analyzer module.

Because this was the first deployment of the system, and because wind conditions at higher elevations in mountainous terrain can differ substantially from those measured in the valley, a conservative flight plan was adopted. The complexity of the terrain, manned helicopter activity, and regulatory constraints made this an unusually difficult flight-planning exercise and far more involved than what is typically required for DIAB operations.

Satellite data

To determine whether Differential InSAR (DInSAR) products could offer regional scale insight into long-term topographical changes, we examined the Canada-wide InSAR vertical deformation map from Samsonov and Feng (2023), which was produced using a fully automated high-performance computing workflow that processed more than 220 000 Sentinel-1 SAR images acquired between 2017 and 2023. As detailed in Samsonov and Feng (2023), the system generated differential interferograms with GAMMA software (Gamma Remote Sensing, Gümligen, Switzerland), removed the topographic phase using the 30 m ASTER DEM, and combined ascending and descending orbit interferograms to derive horizontal and vertical deformation time series across Canada using the multidimensional small baseline subset (MSBAS) technique (Samsonov and d'Oreye, 2012). Uplift from postglacial rebound and tectonic motion signals were filtered from these data to specifically highlight local-scale ground deformation from processes such as landslides (Samsonov and Feng, 2023).

As part of the field campaign, we also tasked SkySat imagery (optical imagery, 30 cm resolution) to capture a recent high-resolution scene of the landslide, offering an updated landscape context to complement our ground and RPAS observations. We also queried the historical archive of RapidEye optical imagery (5 m spatial resolution) spanning from 2009 to 2015 to determine when the landscape changes currently observable at the base of the landslide first emerged. This temporal comparison allowed us to trace the emergence and growth of features such as the debris fan entering the White River, providing valuable long-term context on the evolution of the landslide.

Results

Ground measurements

Fourteen of fifteen wooden stakes, and one metal rebar, originally positioned along the crest of Miles Ridge in 2007 were no longer present in 2025, potentially due to erosion and retreat of the headscarp, snow avalanches, and/or strong winds. Coordinates and horizontal and vertical differences between the 2025 and the original 2007 positions of the one remaining stake (L102 – restaked as L102-new) are shown in Table 1. Table 2 provides the positions of all newly installed MR-series stakes. When the uncertainty of the base station's position is combined with the survey point uncertainties, the resulting uncertainties for the 2025 stake positions are ± 1.8 cm (north), ± 1.6 cm (east) and ± 3.3 cm (vertical).

During the MR-series survey, fresh tension cracks were noted on a vegetated slope near the top of the ridge. Uneven ground surfaces and local subsidence were also visible along the ridge. These features provide evidence of active mass movement and support the interpretation of ongoing instability at the site. Figure 4 illustrates large tension cracks up to approximately 50 cm wide and between 20 and 30 cm deep with relatively fresh roots stretched across the cracks. These observations highlight the importance of integrating GNSS measurements with visual observations to characterize the slope activity at Miles Ridge.

Table 1. Coordinates of stake L102-new as recorded in 2007 and 2025. Horizontal and vertical differences between the coordinates are also shown. HAE is Height Above Ellipsoid. Coordinates displayed in UTM 7N (WGS84).

Stake ID	Material	2007 coordinates (UTM)	2025 coordinates (UTM)	2007 HAE (m)	2025 HAE (m)	Horizontal displacement (m)	HAE difference (m)
L102-new	wooden stake	521937.87E 6871526.56N	521936.57E 6871526.73N	1487.06	1486.97	1.30	-0.090

Table 2. Positions of newly installed MR-series stakes. HAE is Height Above Ellipsoid. Coordinates displayed in UTM 7N (WGS84).

ID	Material	Easting (m)	Northing (m)	HAE (m)
MR - 01	rebar	521686.09	6871731.50	1470.95
MR - 02	wooden stake	521692.43	6871717.19	1469.01
MR - 03	wooden stake	521699.11	6871707.07	1468.64
MR - 04	wooden stake	521704.48	6871698.29	1468.89
MR - 05	wooden stake	521710.20	6871687.22	1470.47
MR - 06	wooden stake	521716.08	6871676.87	1472.46
MR - 07	wooden stake	521721.52	6871666.45	1474.47
MR - 08	wooden stake	521727.67	6871656.06	1477.61
MR - 09	wooden stake	521732.43	6871647.63	1481.50
MR - 10	rebar	521738.62	6871637.14	1483.66
MR - 11	wooden stake	521700.00	6871687.27	1477.79
MR - 12	rebar	521807.06	6871598.86	1480.42

RPAS observations

The imagery collected by the various RPAS flights reveals a variety of surface characteristics and geomorphological zones across various parts of the landslide (Fig. 5). Most of the landslide lacks vegetation, attesting to its high level of ongoing activity, but a vegetated zone does occur in the upper western sector of the landslide (Fig. 5, zone C). In this area, fresh tension cracks were observed, both by RPAS (Fig. 6) and during our ground survey on July 9 (Fig. 4). One set of cracks are located close to the ridge, and a second set occur approximately 40 m downslope where the topography steepens (Fig. 6). The cracks run parallel to the ridge and to the general strike of the rocks which outcrop along the ridge crest.

The upper part of the slide can be divided into three sectors: eastern, centre and northern. In the eastern sector (Fig. 5, zone A), the slide is dominated by rock outcrops which are grey (Kluane ultramafics; Fig. 5, zone A1) to orange brown (Station Creek Formation; Fig. 5, zone A2) in colour. In the centre (Fig. 5, zone B), a broad apron of dark brown talus can be seen, fed by ongoing rockfall from the basalt cliffs above. The western sector (Fig. 5, zone C) comprises the vegetated zone mentioned above. A horizontal view of this upper part of the slide, captured by RPAS, is shown in Figure 7.

The landslide toe comprises a steep light-coloured colluvial apron that is gullied from ongoing seepage and debris flow activity that has mobilized saturated and weathered ultramafic rock from above. On the

Figure 4. *Large tension crack observed just below Miles Ridge. Note the fresh-appearing nature of the debris and the angular rock fragments. Shovel for scale is 100 cm long x 20 cm wide (blade).*

eastern side of the toe, below the craggy outcrops of the Station Creek Formation, fine-grained debris has accumulated in a steep apron with a relatively smooth surface dissected by a nearly straight small gully (Fig. 5, zone D). A larger gully separates this area from a slightly rougher section of the landslide toe to the west (Fig. 5, zone E). Zone E is dissected by a second gully that roughly parallels the larger gully separating zones D and E.

In the central part of the landslide, below the base of the brown basalt talus apron, these two prominent gullies drain from an amphitheatre-shaped scar ~50 m wide that is the source zone for secondary debris flows (hereafter referred to as the 'amphitheatre'; Fig. 5, zone F; Figs. 7 and 8). A dark-coloured lobe (Fig. 5, zone G) is also observed on the northwestern margin of the landslide. This material is assumed to comprise basalt talus which extends further because there are no crags of Station Creek Formation rocks underlying this area of the slide to retain colluvial material mobilized from the headscarp above. Five large angular blocks of dark brown rock several metres in diameter are scattered across this lobe (Fig. 8). These are assumed to be associated with a larger magnitude collapse of a section of the headscarp.

Two drone images of this area captured on July 14 and August 12, 2025 illustrate ongoing erosional processes that occur in the prominent gullies and their associated source zones (Fig. 9). In the July 14 image, a significant volume of brown-coloured debris appears to be filling and possibly clogging the two main gullies, as well as their amphitheatre source zones. By contrast, in the August 12 image, this debris appears to be largely absent from both the channels and the amphitheatres. We speculate that a precipitation event, or events, mobilized this debris and carried it to lower elevations, possibly into the White River.

Figures 10 and 11 illustrate a temporal comparison of the 3D RPAS-derived models collected on July 14 and September 7. The cross-sections in Figure 10a and 10b show approximately 2 m of erosion along a ~13 m section of the eastern margin of the amphitheatre. In contrast, the lower cross-sections in Figure 10c and 10d reveal material deposition within the channel immediately downslope of the amphitheatre, with gains of roughly 2.3 m in depth across the ~11 m wide channel. Additional transects, extracted in both vertical and horizontal orientations across the broader landslide, showed no measurable change over this interval. Figure 11 provides a relative spatial map of the detected surface change at both the slope and amphitheatre scales, highlighting the localized distribution of erosion and deposition. Overall, the amphitheatre exhibits a net gain of 174.4 m³, derived from an estimated 2076.7 m³ of material lost upslope and 2251.2 m³ deposited downslope within the channel.

Satellite measurements

Apparent subsidence of the Miles Ridge landslide area is observed from the Canada-wide active ground deformation DInSAR map data (Fig. 12). These data clearly show negative vertical displacement (i.e., subsidence) rates of up to 2–3 cm/year for most of the landslide area for the 2017–2024 period (Samsonov and Feng, 2023). Confidence in the absolute magnitudes of these data remains tentative as many areas of positive vertical displacement (red [or warm tones] in Fig. 12) are also observed in surrounding areas. While zones of positive vertical displacement

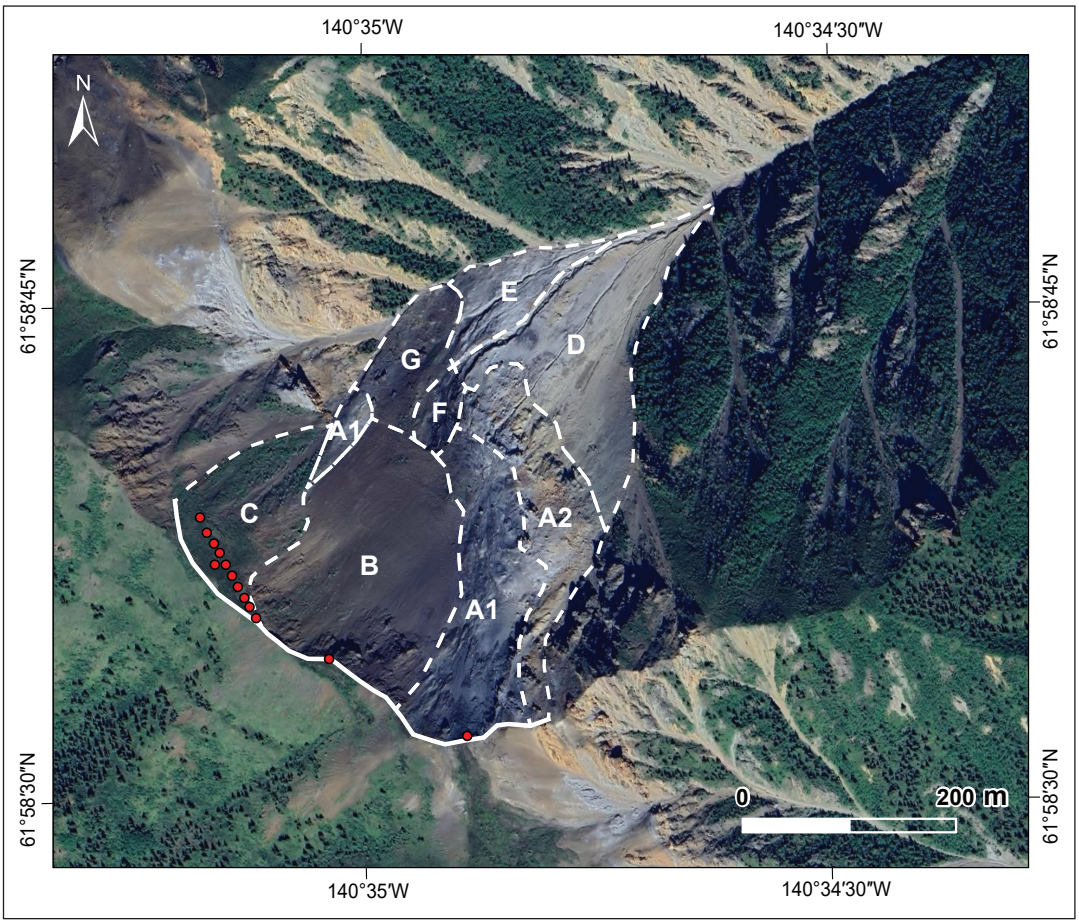

Figure 5. *Geomorphic zones of the Miles Ridge landslide described in the text. Solid white line represents a landslide headscarp located on the ridge crest. Dashed white lines delineate zones. Red points are new stakes that were installed and surveyed on July 9, 2025. The Google Earth background image was acquired on July 4, 2023.*

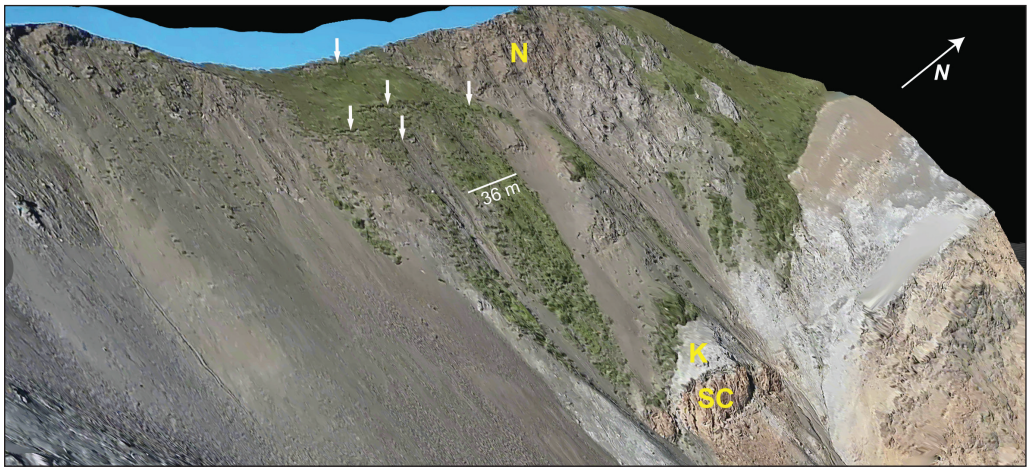

Figure 6. *A 3D RPAS model view displaying tension cracks (white arrows) in the upper vegetated zone of the Miles Ridge landslide. Given the three-dimensional nature of the terrain, the scale bar should be interpreted only for areas lying within the same plane, as distances can be distorted across varying elevations. The main bedrock units are shown as N – Nikolai formation, K – Kluane ultramafics, SC – Station Creek Formation.*

Figure 7. *An RPAS photograph of the landslide.* ***(a)*** *apron of brown talus,* ***(b)*** *smooth lobe,* ***(c)*** *tension cracks,* ***(d)*** *vegetated zones,* ***(e)*** *erosional amphitheatre,* ***(f)*** *highly incised channel,* ***(g)*** *large boulder,* ***(h)*** *dark-coloured lobe,* ***(i)*** *topographically rough lobe.*

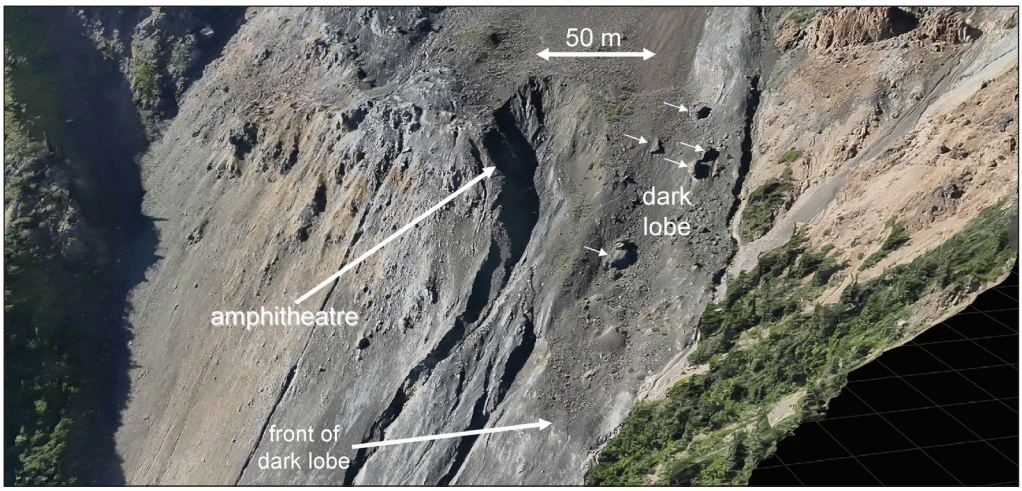

Figure 8. *Detailed view from the August 12, 2025 3D model of the dark-coloured lobe and adjacent amphitheatre. Small white arrows indicate metre-sized rock boulders (largest are 4–6 m in diameter). Given the three-dimensional nature of the terrain, the scale bar should be interpreted only for areas lying within the same plane, as distances can be distorted across varying elevations.*

of up to 3 cm/yr in adjacent areas may be explained by rock glacier movement and floodplain aggradation, we speculate that other, more subtle areas of positive vertical displacement may result from data artefacts. Where holes in the data occur, it is assumed there was either a lack of coherence in ground conditions, or gaps that were not filled by the MSBAS algorithm. Considering that this product has known artefacts and has not yet been formally validated, these findings must be interpreted with appropriate caution.

Finally, based on a Skysat satellite image acquired July 10, 2025, and an orthomosaic of RPAS photographs from July 12, 2025 (Fig. 13), we note that the junction

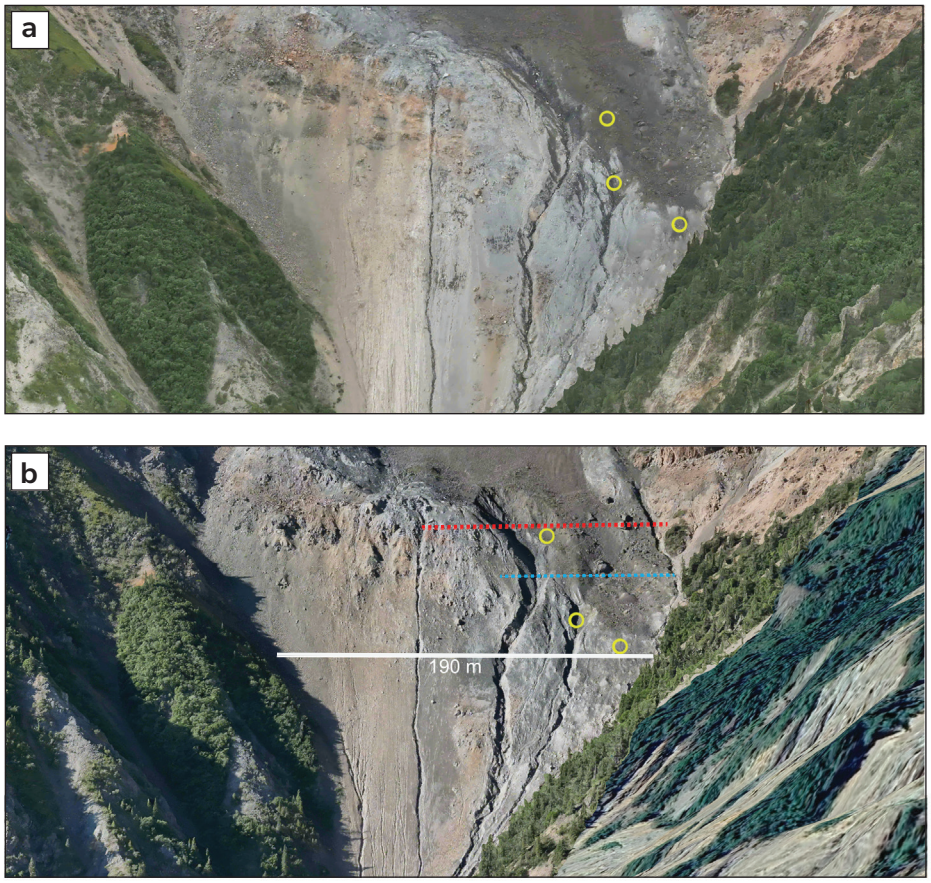

Figure 9. *Two 3D RPAS models showing potential loss of debris from the dark lobe and surrounding erosional features between* ***(a)*** *July 14 and* ***(b)*** *August 12, 2025. Given the three-dimensional nature of the terrain, the scale bar should be interpreted only for areas lying within the same plane, as distances can be distorted across varying elevations. The red and blue dashed lines correspond to the approximate locations of the cross-sections shown in Figure 10. The yellow circles indicate areas where sediment has been lost between the two dates.*

of the landslide drainage channel and the White River, immediately upstream from the bridge, reveals significant debris deposition beyond the immediate margins of the channel. In this area, the forest appears to be partly buried by the large volume of debris. The historical RapidEye imagery acquired between 2009 and 2015 indicates that the debris fan was smaller prior to 2013. The earliest snow-free image, obtained May 15, 2014, reveals further expansion of the fan to approximately its present-day extent (Fig. 13).

Discussion

All but one of the markers installed during the 2007 GPS–GNSS survey on Miles Ridge disappeared or could not be located, likely due to erosion of the ridge crest, snow avalanches, and/or persistent high winds. During the 2025 field campaign, we installed and surveyed a new line of markers just below the ridge (Figs. 2 and 5), providing a modern baseline against which future surveys can assess ground movement in this upper sector of the landslide.

Both our ground survey and our RPAS data revealed a zone of active tension cracks in this upper sector (Figs. 4 and 6). Fresh, vegetation-free soil within the depressions and the presence of fresh roots and angular clasts indicate that these cracks are actively deforming. Future surveys could include repeated measurements of crack width and length, with high-resolution RPAS imagery supporting change detection and aiding in identifying new or expanding fractures.

The upper reaches of the landslide consist of three geomorphic zones. From the southeast to the northwest they are: a sector of rock outcrops, a central talus apron, and a vegetated area containing active tension cracks noted above (Figs. 5 and 7). The central talus zone may be supplying material to the landslide downslope. Mapping moisture patterns in this upper area, using nighttime thermal infrared RPAS surveys, could help identify sections prone to enhanced instability.

The lower reaches of the landslide comprise two main lobes, one relatively smooth on its surface and one relatively rough (Fig. 7). The lobes are incised by several large erosional gullies which originate from

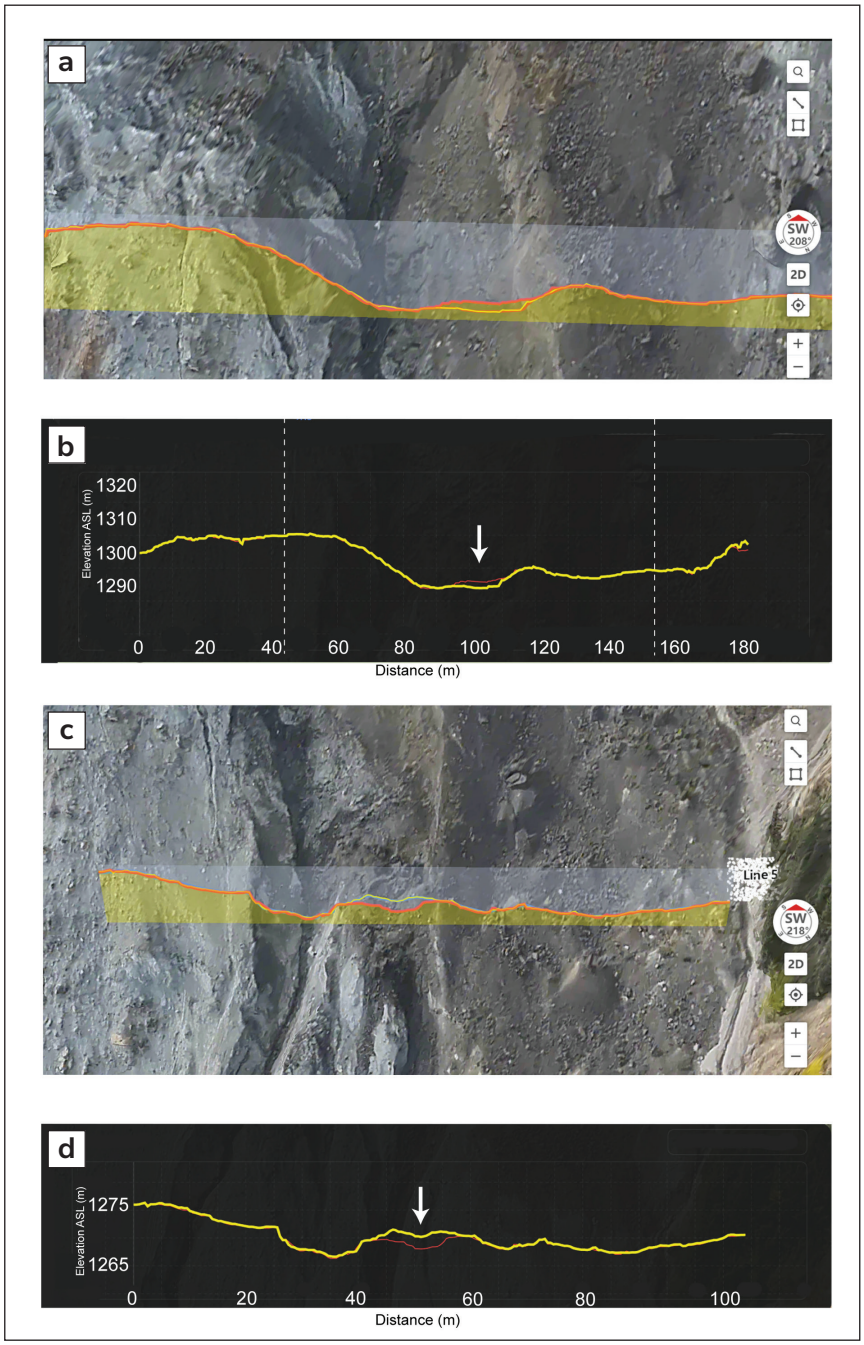

Figure 10. *Comparison of cross-sections across the amphitheatre illustrating areas of material erosion and deposition.* ***(a)*** *Cross-section extracted from the FlightHub 2 3D models showing a zone of erosion between July 14 (red line) and August 12 (yellow line).* ***(b)*** *Elevation-change profile for the same cross-section; the segment between the vertical dashed lines corresponds to the close-up area shown in (a). Arrow indicates area of erosion.* ***(c)*** *Cross-section from the 3D models illustrating a zone of deposition immediately downslope of the amphitheatre over the same time interval.* ***(d)*** *Elevation-change profile for the cross-section shown in (c). Arrow indicates area of deposition.*

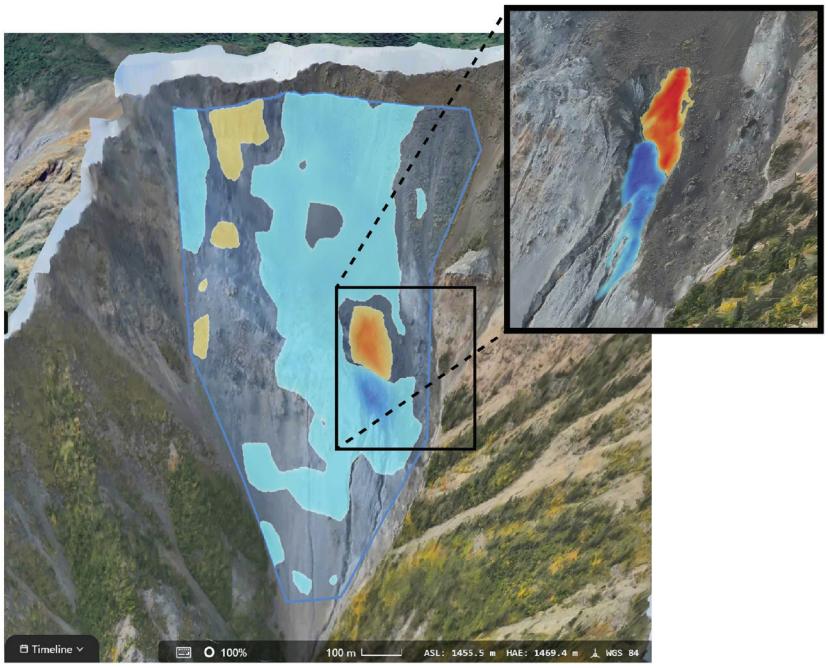

Figure 11. *Relative volume-change map models between July 14 and September 7, 2025, derived from FlightHub 2, where red shading indicates erosion and blue shading indicates deposition. The inset highlights, at higher spatial detail, the two dominant patches exhibiting erosion and deposition, which are associated with the amphitheatre. As of the version released in September 2025 online, volumetric change analyses only provide the total volume change while the spatial map is qualitative only.*

a prominent amphitheatre located in the middle of the landslide. A third prominent dark-coloured lobe is observed on the northern margin of the landslide, adjacent to the amphitheatre and upper gullies (Figs. 7 and 8), and likely receives material from the headscarp above. The amphitheatre and associated region appear to be an area of enhanced erosion, as revealed by our volumetric gain/loss maps (Fig. 11). This can also be seen by the contrasting RPAS imagery of July 14 and August 12, 2025, which suggest erosion of debris, likely during precipitation events (Fig. 9).

To increase spatial detail of the tension cracks near the ridge in future RPAS operations, whether using the Dock 2 or manual flights, two primary approaches can be used. The first is to use the zoom camera, which yields enhanced detail in individual images but cannot support 3D modelling due to the lack of sufficiently accurate geotags. The second is to design flight paths that bring the aircraft closer to the ridge crest, thereby improving the ground-sampling distance. However, this approach increases the likelihood of encountering wind shear or strong local winds associated with daytime anabatic (upslope) and nighttime katabatic (downslope) flows. Conducting RPAS surveys immediately after snowmelt and again prior to snowfall each year would not only provide ground validation for DInSAR deformation estimates but would also supply high-resolution information on the evolution of dynamic geomorphic features such as widening tension cracks and shifting zones of erosion and deposition.

The DInSAR satellite vertical deformation map indicates ongoing localized subsidence across most of the landslide. With continued acquisitions, it may be possible to quantify subsidence rates in different sectors of the landslide, helping to identify zones of acceleration or deceleration and thus assess evolving stability conditions. RapidEye imagery from 2009 to 2015 shows that a major landscape change occurred between 2012 and 2013, during which the debris fan draining into the White River expanded markedly. Notably, the Burwash Landing meteorological station (50 km away) recorded the second-highest annual rainfall on record of 284 mm in 2012 (Kochtitzky et al., 2020), suggesting that unusually wet conditions may have contributed to increased sediment transport during this period. The first cloud-free image from May 15, 2014 reveals that the debris fan had grown further, reaching approximately its present extent (Fig. 13). This expanded fan, characterized by numerous dead and fallen trees, remains evident today in both the SkySat imagery and the RPAS photographs acquired in July 2025. Future analyses could also include digital surface models that can be produced from SkySat stereo pairs or triplets (a single image from a triplet acquired on July 9, 2025 is shown in Figure 13a). Although the resolution is coarser than the RPAS models (metres vs. centimetres), in absence of the Dock 2, these images can be tasked year-round and can provide rapid remote assessments of potential large-scale events or surface changes on the landslide.

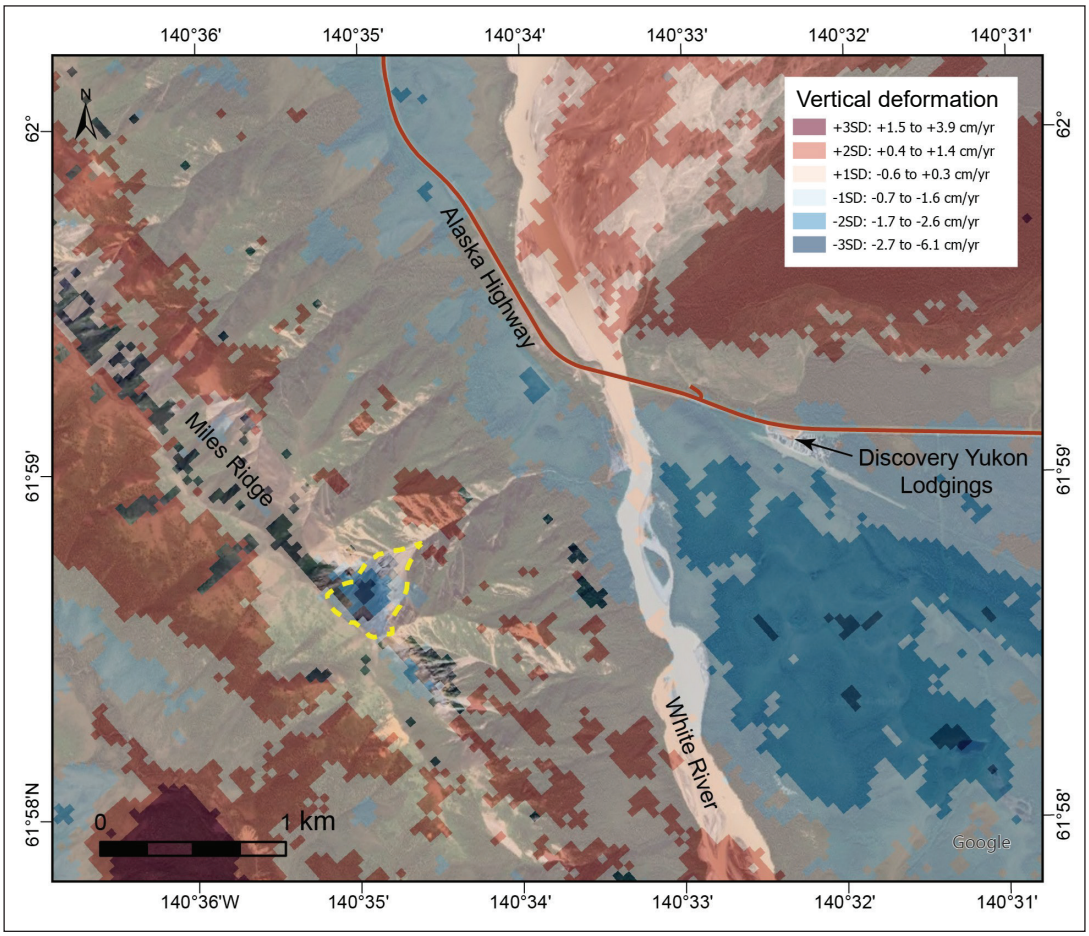

Figure 12. *Annual vertical ground deformation rates measured from InSAR analysis of 2017–2024 Sentinal-1 data (Samsonov and Feng, 2023; Canada Centre for Mapping and Earth Observation, 2024). The Miles Ridge landslide is outlined by the yellow dashed line. The darker blue area south of the Discovery Yukon Lodgings airstrip is interpreted to be subsidence due to the thaw of ice-rich permafrost in glacial drift. The dark red area in the southwest corner is interpreted to be from bulging at the toe of a rock glacier. Google Earth imagery of July 4, 2023 is displayed in the background. Standard deviation classes were generated from a histogram of values observed within a ~25 x 25 km area centred on the White River bridge.*

Concluding remarks

Our integrated ground–RPAS–satellite assessment shows that the Miles Ridge landslide remains a gradually deforming and geomorphically complex system, with localized erosion and deposition in the amphitheatre and continued instability along the ridge crest. Our ground survey documented fresh tension cracks and measurable geomorphic shifts since 2007, while repeated RPAS-derived 3D models revealed focused zones of material loss and accumulation that coincide with the dominant erosional pathways. A vertical deformation map from DInSAR also offers potential for investigating longer-term subsidence patterns across the landslide. Mapping conducted with RPAS offers a promising method for independently validating these DInSAR-derived deformations over multi-year timescales, particularly for small-scale deformation features such as the Miles Ridge landslide, which the national deformation map was originally designed to help monitor.

Given the rapid evolution of DIAB systems, the Dock 2 performed very well during this deployment, demonstrating that semi-autonomous RPAS systems can reliably operate in complex mountainous environments. Newer dock platforms now incorporate built-in battery systems, reducing the need for hard-wired electrical infrastructure and enabling truly mobile deployments from vehicles or semi-permanent field sites. This is an important advance for monitoring remote locations where grid power is unavailable.

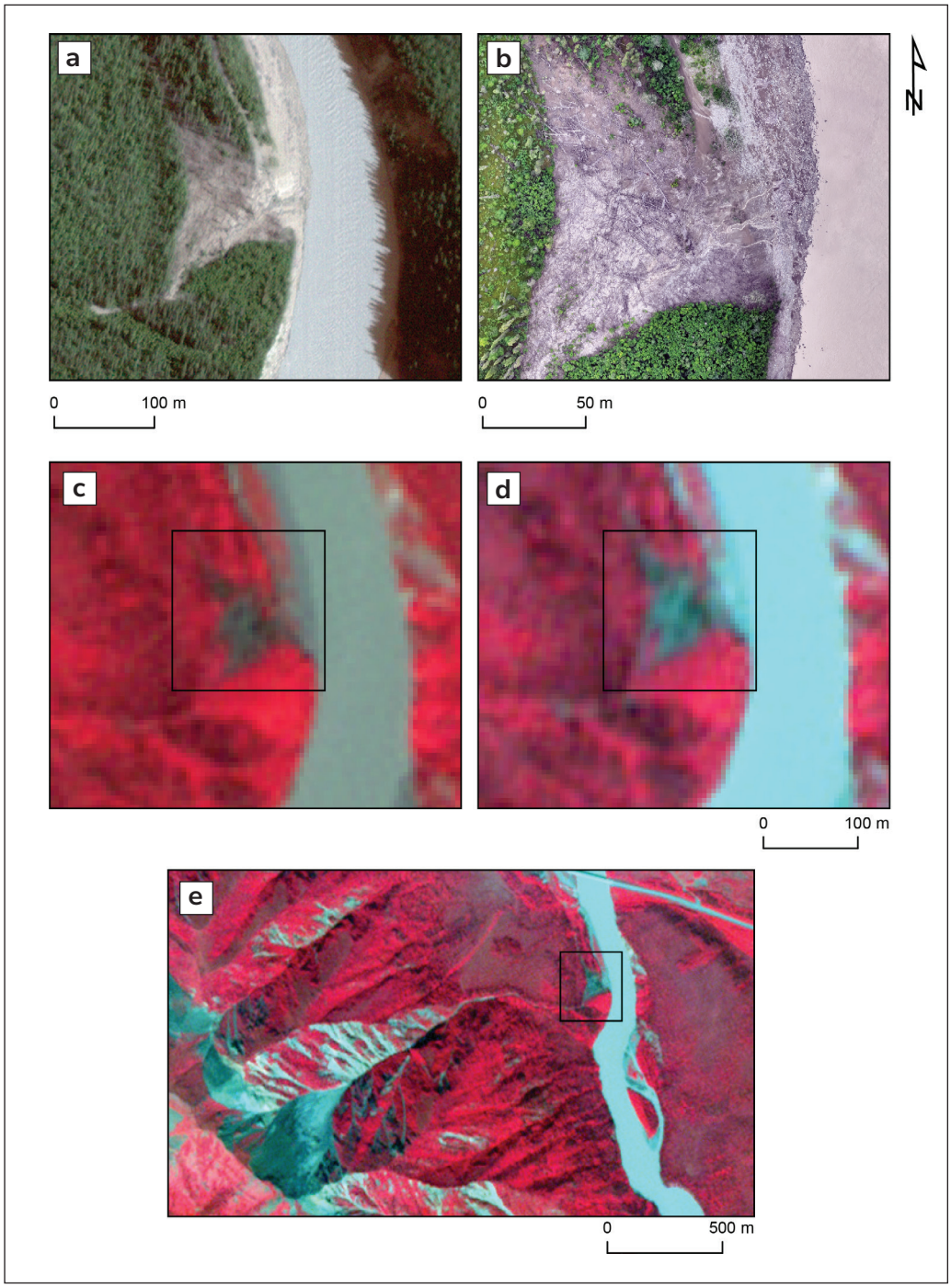

Figure 13. *Change in the extent of the debris fan extending into the White River over time.* ***(a)*** *SkySat satellite image (30 cm pixels) acquired on July 9, 2025, showing the present-day extent.* ***(b)*** *RPAS-derived orthomosaic from July 11, 2025, with a ground sampling distance of 6 cm.* ***(c)*** *RapidEye image acquired on June 28, 2012 (5 m pixels).* ***(d)*** *RapidEye image acquired on July 1, 2013, shown at the same scale as in (c).* ***(e)*** *RapidEye image from June 25, 2015. Panels (a) and (b) are displayed as true-colour RGB composites, whereas panels (c)-(e) use a false-colour NIR–R–G composite to enhance the distinction between vegetation (red tones) and rock/debris (grey tones). Black squares in panels (c)-(e) delineate the location of the debris fan.*

Together, our multiscale observations presented here highlight the ongoing evolution of the Miles Ridge landslide and emphasize the importance of establishing routine monitoring to better evaluate future movement potential and associated risks to the Alaska Highway.

Acknowledgments

This research was funded by the Natural Sciences and Engineering Research Council of Canada (NSERC) Alliance Program grant (grant ALLRP 586350-2), an NSERC Discovery grant (RGPIN-2022-05288) and the Yukon Geological Survey. We thank the Department of Geography, McGill University for access to the RapidEye imagery.

We thank Amanda Harris of Yukon Discovery Lodgings for her enthusiastic and steadfast support of this study, which made this research possible. We also acknowledge the assistance of her staff, in particular Greg Roberts who provided invaluable assistance with the electrical work for the Dock 2 system. We thank Yukon Metals and Capital Helicopters for coordinating flights with us. We also acknowledge Stephen Scheunert and Paul Mondor for access and logistical assistance at a test site in Rigaud, Québec, prior to our Yukon fieldwork. We further acknowledge Kyle Miller formerly from DJI Enterprise and Jason Rule from Transport Canada for help with flight planning. We thank Derek Cronmiller of the Yukon Geological Survey for a helpful review of the manuscript. This work was conducted under the auspices of a Yukon Scientists and Explorers Licence.

References

Bender, A.M. and Haeussler, P.J., 2017. Eastern Denali fault surface trace map, Eastern Alaska and Yukon, Canada. U.S. Geological Survey Open-File Report 2017–1049, 10 p., https://pubs.usgs.gov/of/2017/1049/ofr20171049.pdf.

Blais-Stevens, A., Clague, J.J., Brahney, J., Lipovsky, P., Haeussler, P.J. and Menounos, B., 2020. Evidence for large Holocene earthquakes along the Denali fault in southwest Yukon, Canada. Environmental and Engineering Geoscience, vol. 26, no. 2, p. 149–166, https://doi.org/10.2113/EEG-2263.

Bond, J.D., Lipovsky, P.S. and von Gaza, P., 2008. Surficial geology investigations in Wellesley basin and Nisling Range, southwest Yukon. *In:* Yukon Exploration and Geology 2007, D.S. Emond, L.R. Blackburn, R.P. Hill and L.H. Weston (eds.), Yukon Geological Survey, p. 125–138.

Burn, C.R. and Zhang, Y., 2009. Permafrost and climate change at Herschel Island (Qikiqtaruq), Yukon Territory, Canada. Journal of Geophysical Research Earth Surface, vol. 114, https://agupubs.onlinelibrary.wiley.com/doi/pdf/10.1029/2008JF001087.

Canada Centre for Mapping and Earth Observation, 2024. Pilot national scale maps of active deformation processes in Canada. Natural Resources Canada, Government of Canada, https://app.geo.ca/en-ca/map-browser/record/1da588c1-0dc6-45e4-9e63-9acf2fdc353a [accessed 24/11/2025].

Clague, J.J., 1979. The Denali fault system in southwest Yukon Territory - a geologic hazard? Geological Survey of Canada, Paper No. 79-1A, p. 169–178, https://doi.org/10.4095/104844.

Finley, T., Salomon, G., Stephen, R., Nissen, E., Cassidy, J. and Menounos, B., 2022. Preliminary results and structural interpretations from drone lidar surveys over the Eastern Denali fault, Yukon. *In:* Yukon Exploration and Geology 2021, K.E. MacFarlane (ed.), Yukon Geological Survey, p. 83–105.

Gariano, S.L. and Guzzetti, F., 2016. Landslides in a changing climate. Earth-Science Reviews, vol. 162, p. 227–252, https://doi.org/10.1016/j.earscirev.2016.08.011.

Government of Canada, 2025. Precise point positioning, http://webapp.csrs-scrs.nrcan-rncan.gc.ca/geod/tools-outils/ppp.php [accessed 19/11/2025].

Haeussler, P.J., Matmon, A., Schwartz, D.P. and Seitz, G.G., 2017. Neotectonics of interior Alaska and the late Quaternary slip rate along the Denali fault system. Geosphere, vol. 13, no. 5, p. 1445–1463, https://doi.org/10.1130/GES01447.1.

Han, J., Dettmer, J., Gosselin, J.M., Gilbert, H., Biegel, K. and Kim, S., 2024. Seismicity near the eastern Denali fault from temporary and long-term seismic recordings. *In:* Yukon Exploration and Geology Technical Papers 2023, L.H. Weston and Purple Rock Inc. (eds.), Yukon Geological Survey, p. 37–50.

Hirabayashi, Y., Mahendran, R., Koirala, S., Konoshima, L., Yamazaki, D., Watanabe, S., Kim, H. and Kanae, S., 2013. Global flood risk under climate change. Nature Climate Change, vol. 3, no. 9, p. 816–821, https://doi.org/10.1038/nclimate1911.

Holland, G. and Bruyère, C.L., 2014. Recent intense hurricane response to global climate change. Climate Dynamics, vol. 42, no. 3, p. 617–627, https://doi.org/10.1007/s00382-013-1713-0.

Irrgang, A.M., Lantuit, H., Manson, G.K., Günther, F., Grosse, G. and Overduin, P.P., 2018. Variability in rates of coastal change along the Yukon coast, 1951 to 2015. Journal of Geophysical Research Earth Surface, vol. 123, no. 4, p. 779–800, https://doi.org/10.1002/2017JF004326.

Kalacska, M., Lucanus, O., Arroyo-Mora, J.P., Stix, J., Lipovsky, P. and Roman, J., 2026. Assessing a semi-autonomous drone-in-a-box system for landslide monitoring: A case study from the Yukon Territory, Canada. Sustainability, vol. 18, no. 2, https://doi.org/10.3390/su18020693.

Kochtitzky, W., Winski, D., McConnell, E., Kreutz, K., Campbell, S., Enderlin, E.M., Copland, L., Williamson, S., Main, B. and Jiskoot, H., 2020. Climate and surging of Donjek glacier, Yukon, Canada. Arctic, Antarctic, and Alpine Research, vol. 52, no. 1, p. 264–280, https://doi.org/10.1080/15230430.2020.1744397.

Marechal, A., Ritz, J.-F., Ferry, M., Mazzotti, S., Blard, P.-H., Braucher, R. and Saint-Carlier, D., 2018. Active tectonics around the Yakutat indentor: New geomorphological constraints on the eastern Denali, Totschunda and Duke River faults. Earth and Planetary Science Letters, vol. 482, p. 71–80, https://doi.org/10.1016/j.epsl.2017.10.051.

Munich RE, 2025. Natural disasters worldwide: losses are on the rise as climate change strikes, https://www.munichre.com/en/risks/natural-disasters.html [accessed 23/11/2025].

Samsonov, S. and d'Oreye, N., 2012. Multidimensional time-series analysis of ground deformation from multiple InSAR data sets applied to Virunga Volcanic Province. Geophysical Journal International, vol. 191, no. 3, p. 1095–1108, https://doi.org/10.1111/j.1365-246X.2012.05669.x.

Samsonov, S.V. and Feng, W., 2023. Deformation retrievals for North America and Eurasia from Sentinel-1 DInSAR: Big data approach, processing methodology and challenges. Canadian Journal of Remote Sensing, vol. 49, no. 1, https://doi.org/10.1080/07038992.2023.2247095.